Overview of SIDIS results from Hall B at Jefferson Lab

H. Avakian[1]
(The CLAS Collaboration)
[1] Thomas Jefferson National Accelerator Facility, Newport News, Virginia 23606
(Dated: January 31, 2017)

We present studies of spin and azimuthal asymmetries in pion production in semi-inclusive deep inelastic scattering (SIDIS), using the data sets from the CEBAF Large Acceptance Spectrometer (CLAS) at Jefferson Lab with polarized NH_3 and unpolarized hydrogen targets. Three run periods, e1-6, e1-f and eg1-dvcs used respectively 5.7, 5.5 and 5.8 GeV longitudinally polarized electron beam and unpolarized liquid hydrogen (e1-6, e1-f) and polarized NH_3 (eg1-dvcs) targets. Pion channels (π^+, π^-, π^0) were studied over a broad kinematical range ($x = 0.1 - 0.6$, $Q^2 = 1.0 - 4.5$ GeV^2, $z = 0.0 - 1.0$, $P_{h\perp}^2 = 0.0 - 1.0$ GeV^2, and $-180^\circ < \phi < 180^\circ$). These measurements give insights into the transverse momentum dependence of parton distribution functions (PDFs) for different polarization states, describing the dynamics of quarks and gluons inside of the proton.

Semi-inclusive deep-inelastic scattering (SIDIS) has emerged as a powerful tool to probe nucleon structure and to provide access to Transverse Momentum Dependent (TMD) partonic distributions through measurements of spin and azimuthal asymmetries. A SIDIS ($\ell(k) + N(P) \to \ell'(k') + h(P_h) + X(P_X)$) reaction is one in which a beam lepton, ℓ with the 4-momenta k, scatters off of a target nucleon, N, via the exchange of a photon and the scattered lepton, ℓ', is detected along with a single hadron, h with 4-momenta P_h; everything else in the final state, X, is ignored.

Assuming single photon exchange, the leptoproduction cross-section can be written as a sum of several azimuthal modulations coupled to corresponding structure functions. In case of the longitudinally polarized beam and target it has following contribution (see [1]):

$$\frac{d^5\sigma}{dx\; dQ^2\; dz\; d\phi\; dP_{h\perp}^2} \propto F_{UU,T} + \varepsilon F_{UU,L} + \sqrt{2\varepsilon\,(1+\varepsilon)}\cos\phi F_{UU}^{\cos\phi} + \varepsilon\cos(2\phi)\, F_{UU}^{\cos 2\phi} + \lambda_e\sqrt{2\varepsilon\,(1-\varepsilon)}\sin\phi F_{LU}^{\sin\phi}$$
$$+S_{||}[\sqrt{2\varepsilon\,(1+\varepsilon)}\sin\phi F_{UL}^{\sin\phi} + \varepsilon\sin(2\phi)\, F_{UL}^{\sin 2\phi} + \lambda_e(\sqrt{1-\varepsilon^2}F_{LL} + \sqrt{2\varepsilon\,(1-\varepsilon)}\cos\phi F_{LL}^{\cos\phi})], \quad (1)$$

where structure functions $F_{...}^{...}$ [1] depending on kinematical variables $x, Q^2, z, P_{h\perp}$ are corresponding azimuthal moments, and the azimuthal angle ϕ is the angle between the lepton plane and the hadron production plane. The kinematic variables x, y, and z are defined as: $x = Q^2/2(P\cdot q)$, $y = (P\cdot q)/(P\cdot k)$, $z = (P_h\cdot P)/(P\cdot q)$, where $Q^2 = -q^2 = -(k-k')^2$ is the squared four-momentum of the virtual photon, and $P_{h\perp}$ is the transverse momentum of the detected hadron. The ratio ε of the longitudinal and transverse photon flux is given by: $\varepsilon = \frac{1-y-\gamma^2y^2/4}{1-y+y^2/2+\gamma^2y^2/4}$, where $\gamma = 2Mx/Q$, and M is the nucleon mass.

The structure functions could be presented as a convolution of different PDFs, and fragmentation functions (FFs). For example $F_{UU,T}$ and F_{LL} will be described by convolutions of f_1 and g_1 twist-2 PDF and D_1 fragmentation function, with $F_{UU,T} \simeq \mathcal{C}\,[f_1 D_1]\,, F_{LL} \simeq \mathcal{C}\,[g_1 D_1]$, where $\mathcal{C}$ stands for convolution (Eq. 4.1 of of Ref. [1]).

Most of the structure functions involve transversely polarized quarks. For example the $F_{UU}^{\cos 2\phi}$, at leading twist can be presented as a convolution of Boer-Mulders distribution function, $h_1^\perp$ describing the correlation between the transverse motion of a quark and its own transverse spin [2], and the Collins fragmentation function, $H_1^\perp$ [3], describing fragmentation of transversely polarized quarks.

Some of the structure functions, although, suppressed by $P_{h\perp}/Q$ (for example cosine modulation (known as the Cahn effect [4]), appeared to be significant and dominating in the $P_{h\perp}$ ∼1 GeV range. Additional contribution to $\cos\phi$ and $\cos 2\phi$ moments coming from processes when the final meson is produced at short distances via hard-gluon exchange [5] may also be significant in the kinematic regime where the ejected meson carries most of the virtual photon momentum (z approaching 1). It appeared that the interplay between the parton transverse momentum and spin (Boer-Mulders effect [2]) can also generate sub leading contribution to $\cos\phi$. The $F_{UU}^{\cos\phi}$ receive contribution from the convolution of twist-2 and twist-3 distribution and fragmentation functions, such as the twist-3 h related to Boer-Mulders DF $h_1^\perp$ ([2, 6]), the Collins FF $H_1^\perp$, and the twist-3 DFs h and $f^\perp$ [1]. The higher-twist observables are a key for understanding long-range quark-gluon dynamics. They have also been interpreted in terms of average transverse forces acting on a quark at the instant after absorbing the virtual photon [7].

In the Wandzura-Wilczeck approximation [8] only two contributions are considered:

$$F_{UU}^{\cos\phi} \;\simeq\; -\frac{2M}{Q}\;\mathcal{C}\left[\frac{\vec{P}_{h\perp}\cdot\vec{k}_\perp}{MP_{h\perp}}xf^\perp D_1 + \frac{\vec{P}_{h\perp}\cdot\vec{p}_\perp}{zM_hP_{h\perp}}xhH_1^\perp\right], \quad (2)$$

where the first (second) term is related to the Cahn (Boer-Mulders) effect [1] and $\vec{k}_\perp$ and $\vec{p}_\perp$ are quark transverse momenta in the initial and final state. Several measurements of cosine modulations in semi-inclusive DIS experiments have been published in the past [9–12]. Significant cosine modulations with azimuthal angle, ϕ, observed in various experiments indicate that higher-twist effects can be very important.

The HERMES experiment measured cosine modulations of hadrons produced in the scattering of 27.5 GeV/c electrons and positrons off pure hydrogen and deuterium targets, where the lepton beam scatters directly off neutrons and protons (with only negligible nuclear effects in case of deuterium) [13]. For the first time these modulations were determined in a four-dimensional kinematic space for positively and negatively charged pions and kaons separately, as well as for unidentified hadrons. At COMPASS, positive and negative hadrons produced by the 160 GeV/c muon beam scattering off a ^{6}LiD target have been measured in a three-dimensional grid of the relevant kinematic variables x, z and $P_{h\perp}^2$ [14]. In all the experiments, the new data confirm the existence of a sizable $\cos\phi$ and a non-zero $\cos 2\phi$ modulations.

The azimuthal modulations have been studied phenomenologically in detail, also using phase space limitations due to finite beam energies of real experiments [15]. The cosine modulation in particular is most sensitive to transverse momentum distributions leading to significant corrections due to limitation of the phase space in experiments.

I. CLAS CONFIGURATIONS

In the following we discuss three data sets from CLAS at JLab. Scattered electrons were detected in CLAS using a coincidence of the gas Cherenkov counters and the lead-scintillator electromagnetic calorimeter [16]. Polarized target runs (eg1-dvcs) also used the CLAS inner calorimeter, improving detection of neutrals at small angles (Fig. 1). Deep-inelastic scattering events were selected by requiring $Q^2 > 1$ GeV^2 and $W > 2$ GeV, where W is the invariant mass of the hadronic final state. A minimum value for the final state pion transverse momentum, $P_{h\perp} > 0.05$ GeV, ensures that the azimuthal angle ϕ is well-defined. The total number of selected $e\pi$ coincidences was $\approx$ 7M, 6M and 4M for e1-f, e1-6 and eg1-dvcs data sets for the presented z range, $0.4 < z < 0.7$, which selects the semi-inclusive region [17]. Events with missing-mass values for the $e\pi X$ system that are smaller than 1.4 GeV ($M_X(e\pi)$ <1.4 GeV) were discarded to suppress contributions from exclusive processes, such as $ep \to e\pi N$, and $ep \to e\pi\Delta$. The average beam polarization during the data taking was $\sim 75\%$, and the average target polarization of protons ($^{14}NH_3$) for polarized target run was $\sim 80\%$.

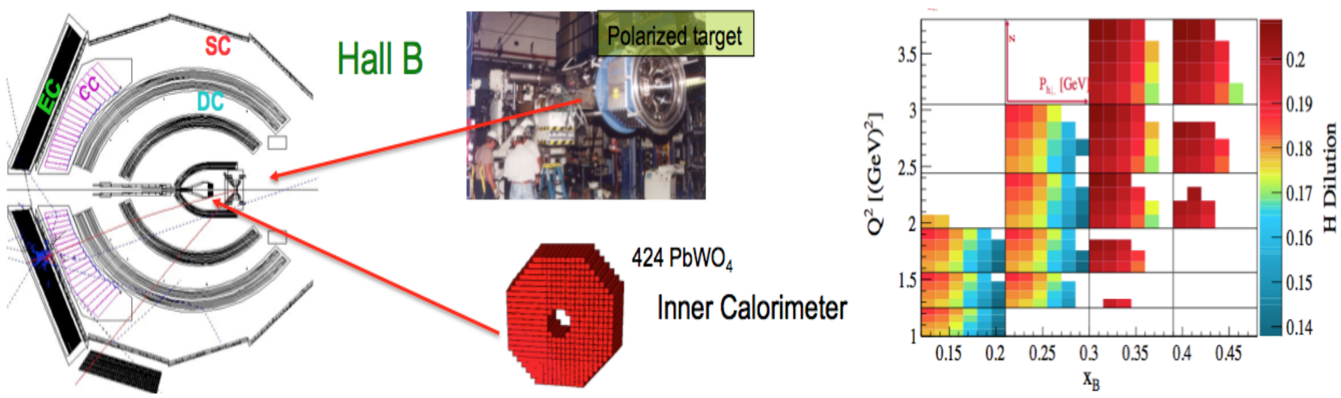

FIG. 1: (color online) CLAS detector components, EC-Electromagnetic Calorimeter, CC-Cherenkov Counter, DC- Drift Chamber (3 regions), and time of flight Scintillators (SC). The right plot shows the kinematical coverage in x-Q^2 and the dilution factor (see the text) in z-$P_{h\perp}$ bins for $ep \to e'\pi^+X$.

II. AZIMUTHAL ASYMMETRIES FROM UNPOLARIZED TARGET

Studies of transverse momentum distributions using the SIDIS multiplicities [18] indicate wide spread of the values for average transverse momentum of quarks due to experimental errors. The main challenge in extraction of ϕ distributions of hadrons in SIDIS is the handling of the detector acceptance, both geometrical acceptance (the location of active detector elements) and the efficiency in the active regions. For a given kinematical bin, the acceptance is defined as the ratio of the number of reconstructed events (using a GEANT based simulation of the CLAS detector)

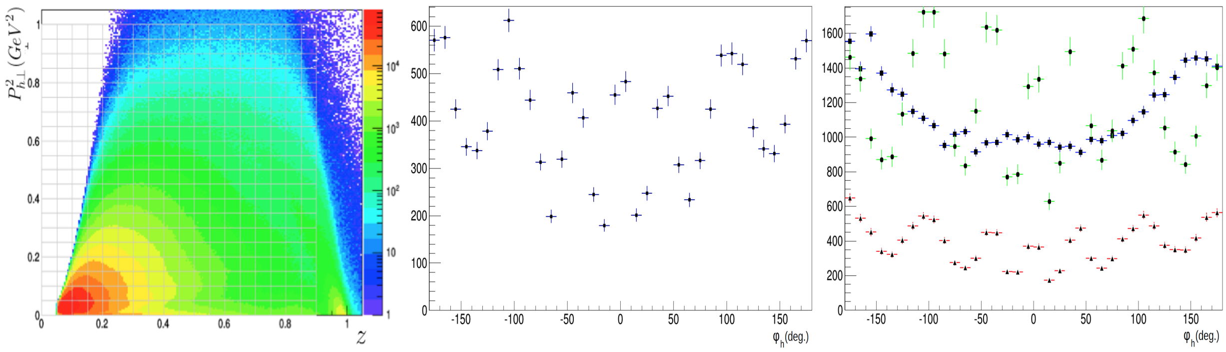

FIG. 2: (color online) Distributions in $P_{h\perp}$ and z for positive pions (left), dependence on azimuthal angle ϕ (π^+ channel) of observed counts (middle); Monte Carlo (right) - generated (blue squares), reconstructed (red triangles), and acceptance (green circles) (acceptance scale goes from 0.0 - 0.5) for a given bin in x, Q^2, z, and $P^2_{h\perp}$ ($0.2 < x < 0.3$, $1.3 < Q^2 < 1.7 GeV^2$, $0.4 < z < 0.45$, $0.4 < P^2_{h\perp} < 0.45$ GeV^2).

to the number of generated events. The main corrections included bin centering corrections and radiative corrections calculated using the HAPRAD version 2.0 [19, 20]. A table of values of normalized counts in elementary bins has been extracted in 5-dimensional bins in $x, Q^2, z, P_{h\perp}$ and ϕ [21]. The kinematical distributions of final state pions and corresponding ϕ-distributions from detector, and corresponding inefficiencies extracted from MC simulation are illustrated in Fig. 2. In order to extract azimuthal moments, and in view of future extraction of multiplicities, the ϕ (unpolarized) distributions of charged pions yields (corrected as mentioned above) for each $x - Q^2 - z - P^2_{h\perp}$ bin are fit with the function $A_0(1 + A^{\cos\phi}_{UU} \cos\phi + A^{\cos 2\phi}_{UU} \cos 2\phi)$. A representative plot is shown here in Fig 3, which shows A_0 and $A^{\cos\phi}_{UU}$ vs $P^2_{h\perp}$ for one z bin for both pion channels.

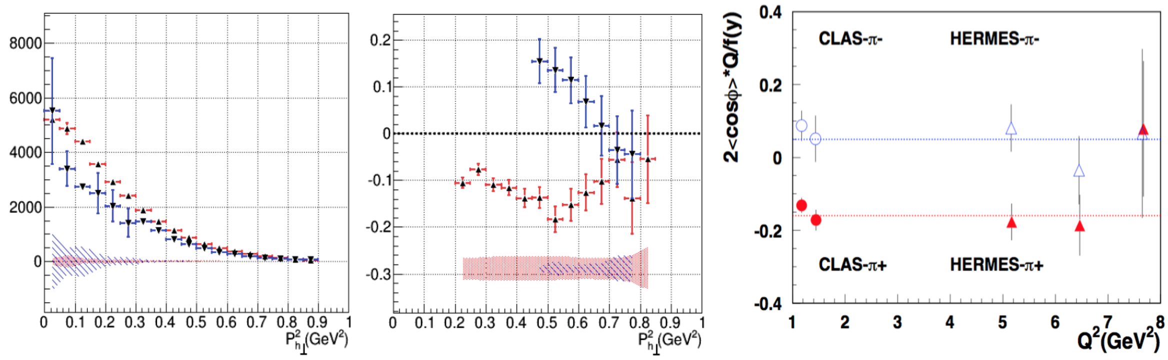

FIG. 3: (color online) CLAS e1-f preliminary results [21] with A_0 (left), $A^{\cos\phi}_{UU}$ (middle) for the π^+ (red upward pointing triangles) and π^- (blue downward pointing triangles) channels as a function of $P^2_{h\perp}$ for the high Q^2 bin of $0.2 < x < 0.3$ and $0.4 < z < 0.45$. The right panel shows he $\cos\phi$ modulations in $\pi^\pm$ SIDIS plotted vs Q^2 for a bins with $x \approx 0.19$, and $z \approx 0.35, P_{h\perp} \approx 0.6$ GeV (left). Filled symbols are for π^+ and open symbols for π^-. The circles are for CLAS and the triangles for HERMES [13].

The moments extracted for π^+ channel show good agreement, both qualitatively and quantitatively with the similar measurement published by the CLAS Collaboration using e1-6 data [22], implying good consistency between measurements.

The cosϕ asymmetry gets contributions only at sub-leading twist and can be used to constrain the related terms [4, 5, 23]. The formalism based on the twist-3 approach could be tested in Q^2dependence of $\cos\phi$ modulations. In the Fig. 3 CLAS measurements are also compared with corresponding measurements from HERMES experiment [13], after taking into account the kinematic factors in the expression of the $\cos\phi$ modulation and ϕ independent terms ([1]), with $f(y) = \sqrt{2\epsilon(1+\epsilon)}$. The CLAS and HERMES measurements are found to be consistent with each other in a wide range of Q^2, as shown in Fig. 3, indicating that at energies as low as 5-6 GeV, the behavior of azimuthal modulations are similar to higher energy measurements. For comparison, the lowest x CLAS bin and highest x HERMES bins were used with equal average values of x, z and $P_{h\perp}$. The CLAS data provide significant improvements in the precision of azimuthal moments for the kinematic region where the two data sets overlap, and they extend the measurements to the large x region not accessible at HERMES.

Difference in the beam energy may also provide additional information on phase space limitation effects on corresponding observables. Our studies using MC simulation of Cahn and Boer-Mulders contributions, assuming Gaussian distributions from Ref.[15], indicate that phase space limitations may have very different effects on them. The Fig. 4 shows the effects of accounting the maximum possible transverse momentum of quarks (assuming on-shell quarks) on the magnitude of the $\cos\phi$-moment from two competing contributions. If the underlying assumptions could be validated, that will indicate significant suppression of azimuthal asymmetries generated at distribution level (e.g. Cahn).

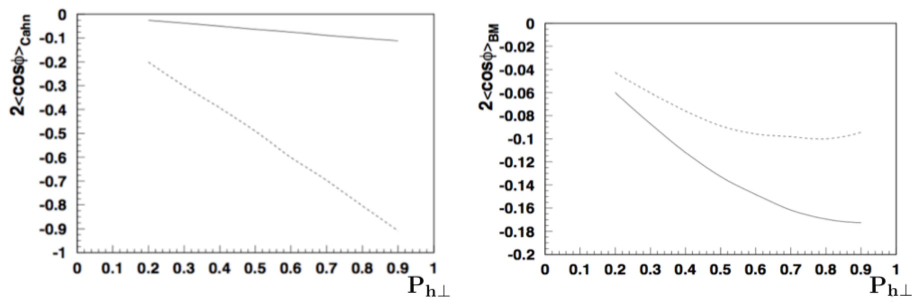

FIG. 4: The $\cos\phi$ modulations in π^+ production in SIDIS for beam energy 5.5 GeV, plotted vs $P_{h\perp}$ for $x = 0.19$, and $z = 0.5$ for Cahn (right) and Boer-Mulders (left) contributions. The dashed lines show the predictions for integrating Eq. 2 over quark transverse momentum up to infinity, and solid line shows the effect of integrating it to a maximum value defined by additional assumptions on conservation of total energy of the system and forward direction of the scattered quarks discussed in Ref.[15]

III. STUDIES OF THE SPIN ASYMMETRIES WITH POLARIZED TARGET

The studies of SIDIS with polarized ammonia, requires separation of events from free protons from unpolarized bound nucleons. The main goal of this experiment was the extraction of Single Spin Asymmetries (SSAs) and Double Spin Asymmetries (DSAs) in fine bins in x and $P_{h\perp}$. The understanding the dilution factor, fraction of polarized nucleons (N) to unpolarized material, is a major effort in precision multidimensional analysis, for multiparticle final states. The dilution factor defined as $f_{DF} = \rho_N l_N \sigma_N / \sum_i \rho_i l_i \sigma_i$, where ρ, l and σ are densities of the target materials, their lengths and the SIDIS event cross sections, respectively, is shown as a function of x for different $P_{h\perp}$ bins in Fig. 5 for neutral pions.

The double-spin asymmetries extracted from eX sample ($A_1^p(eX)$) and from π^0 SIDIS ($A_1^p(e\pi^0 X)$) at relatively large values of x, where valence quarks dominate, in a simple parton model are consistent with each other and can be described by $\approx (4\Delta u + \Delta d)/(4u + d)$. A comparison of the extracted DSA, A_{LL}, for π^0 integrated over z, $P_\perp$, ϕ and Q^2, and divided by the depolarization factor [24] with the ratio g1/F1 of inclusive structure functions (from the same eg1-dvcs experiment [24]) are shown in Fig. 5.

The measurements of the double spin asymmetry as a function of the transverse momentum of hadrons provides important information on transverse momentum distributions of polarized quarks. Large acceptance of CLAS for neutral pions, provided by the CLAS inner calorimeter, allows measurements of SSAs and DSAs in multidimensional bins, with negligible correlation between x and $P_{h\perp}$ (see Fig. 5), crucial for studies of transverse momentum dependent effects. Latest calculations by Bourrely and Soffer [25] using their statistical approach with additional transverse momentum dependence of parton distributions, predict some rise of the double-spin asymmetry with $P_{h\perp}$.

IV. BACK-TO-BACK HADRON PRODUCTION IN SIDIS

Detection of two hadrons in SIDIS provides a unique possibility to access the details of quark gluon interactions inaccessible in single-hadron SIDIS. Large acceptance of the CLAS detector at Jefferson Lab, allowing detection of two hadrons, produced back-to-back (b2b) in the current and target fragmentation regions, provides a unique possibility to study the nucleon structure in target fragmentation region (TFR), and correlations of target and current fragmentation regions. The production of two hadrons in polarized SIDIS, with one spinless hadron produced in the current fragmentation region (CFR) and another in the TFR, would provide access to the full set of leading twist

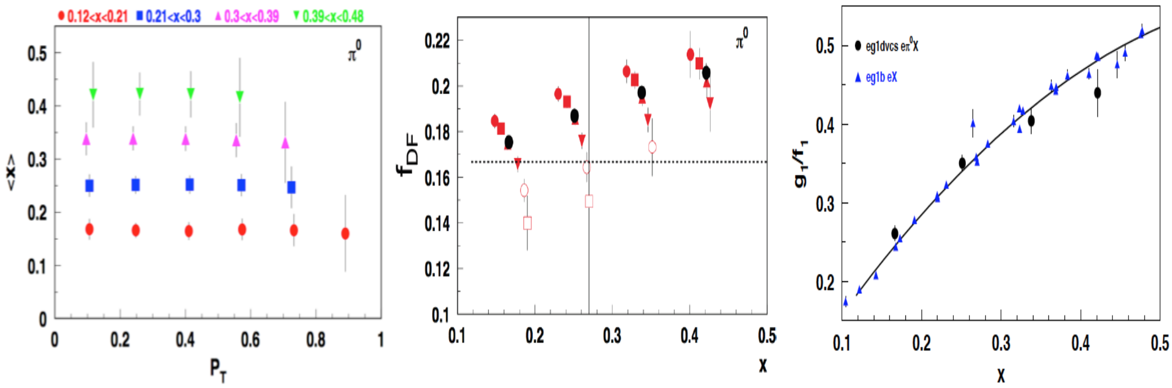

FIG. 5: (color online) CLAS eg1-dvcs preliminary results: The average x for different values of the transverse momentum (left), the dilution factor for π^0 (middle) and the g_1/f_1 versus x for π^0 compared with CLAS inclusive measurements [24] (right). The depolarization factor (Eq. 2 from Ref. [17] has been calculated assuming using R = 0.1 for the ratio of longitudinal to transverse photon cross sections.

fracture functions [26]. The leading twist formalism for spin and transverse-momentum dependent fracture functions, describing conditional probabilities to produce a hadron of certain type in a target fragmentation for a given flavor of struck quark has been developed in Refs. [26, 27].

For an unpolarized target expressions there are two contributions σ_{UU} and σ_{LU}, involving convolutions of unpolarized, longitudinally and transversely polarized quark fracture functions (see Fig. 6) and fragmentation functions of unpolarized, D_1, and transversely polarized quarks, $H_1^\perp$, [27]:

$$\sigma_{UU} = F_0^{\hat{u}\cdot D_1} + \ldots, \; \sigma_{LU} = -\frac{P_{T1}P_{T2}}{m_2 m_N} F_{k1}^{\hat{l}^{\perp h}\cdot D_1} \sin(\phi_1 - \phi_2)\,, \tag{3}$$

In the valence-quark region ($x > 0.1$) accessible at JLab with CLAS detector at 5.7 GeV the polarization transfer from the beam is expected to be significant. High luminosity and high polarization of the electron beam makes CLAS an ideal place for studies of correlations between target and current fragmentation regions. The measurements of single spin asymmetry defined by Eq.3 in semi-inclusive production of protons and charged pions in coincidence with the scattered electron in hard scattering kinematics ($Q^2 > 1$ GeV^2, $W^2 > 4$ GeV^2) have been performed by the CLAS Collaboration using 5.5 GeV and 5.7 GeV longitudinally polarized electron beams scattering off a 5-cm-long liquid-hydrogen target (CLAS e1-f and e1-6 experiments). Significant single-spin asymmetries have been observed in back-to-back pion and proton electroproduction for the first time [28]. The transverse momentum dependence of the SSA shows a trend for asymmetry to increase with increasing transverse momenta of pion and proton P_{T1},P_{T2}, consistent with expectations from theory.

Target and current fragmentation regions were selected by cuts on the x_F variables of protons ($x_F < 0$) and pions ($x_F > 0$), in addition to standard data quality, vertex, acceptance,and fiducial cuts. Based on previous studies we have chosen $0.4 < z < 0.7$ as the canonical cut on the final state π^+ to exclude contamination from exclusive events and decay pions from baryon resonances produced in the target fragmentation region. With a cut on the missing mass of the $e'\pi^+X$ system, $M_X > 1.4$ GeV we have almost no data at $z > 0.7$, but we use this cut as it was determined in Hall C that strong deviations for the quark-parton model occur at high z [29]. The contamination from target fragmentation, higher twists, or other effects are important for $z < 0.3$.

V. CONCLUSIONS

In summary, we have presented measurements of the kinematic dependences of the spin-azimuthal modulations in semi-inclusive pion electroproduction from three CLAS data sets, indicating significant dependence of observables on the flavor of final state. The target and beam-target asymmetries from neutral pion electroproduction in deep-inelastic scattering have been measured as a function of $P_\perp$, providing access to transverse momentum distributions of longitudinally polarized quarks. The results for $\cos\phi$-moment are compared with published HERMES data [13], providing a significant improvement in precision and can serve as an important input for studies of higher-twist effects. The Q^2-dependence of the $\cos\phi$ modulation is consistent with the twist-3 nature of the contribution and within statistical uncertainties is consistent with measurements performed at much higher energies and Q^2. Higher precision data from 12 GeV running of JLab will be required to study the Q^2-dependence of observables in more

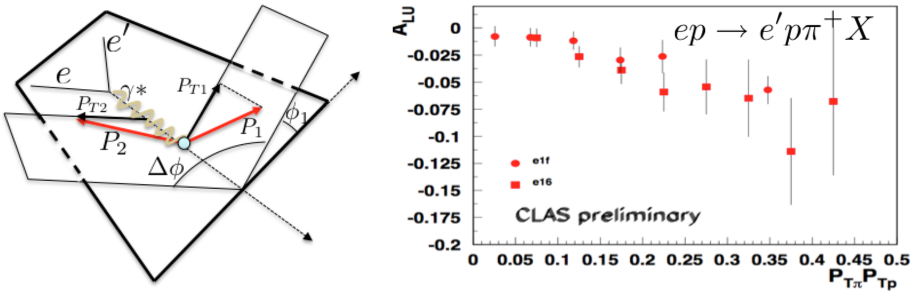

FIG. 6: The kinematic plane for back-to-back (b2b) hadron production in SIDIS (left) and comparison of the single-spin asymmetry measurements from two run periods (e1-6 square symbols and e1-f circles), for b2b production of π^+ and proton (right) .

details. A non-zero A_{LU} in b2b SIDIS indicate that spin-orbit correlations between hadrons may be very significant, opening a new avenue for studies of the complex nucleon structure in terms of quark and gluon degrees of freedom.

This material is based upon work supported by the U.S. Department of Energy, Office of Science, Office of Nuclear Physics under contract DE-AC05-06OR23177.

[1] A. Bacchetta *et al.*, JHEP **02**, 093 (2007), `arXiv:hep-ph/0611265` .
[2] D. Boer and P. J. Mulders, Phys. Rev. **D57**, 5780 (1998), `hep-ph/9711485` .
[3] J. C. Collins, Nucl. Phys. **B396**, 161 (1993), `hep-ph/9208213` .
[4] R. N. Cahn, Phys. Lett. **B78**, 269 (1978).
[5] E. L. Berger, Z. Phys. **C4**, 289 (1980).
[6] B. Pasquini and F. Yuan, Phys. Rev. **D81**, 114013 (2010), `arXiv:1001.5398[hep-ph]` .
[7] M. Burkardt, hep-ph **0807.2599** (2008), `arXiv:hep-ph/0807.2599[hep-ph]` .
[8] S. Wandzura and F. Wilczek, Phys. Lett. **B72**, 195 (1977).
[9] J. J. Aubert *et al.* (European Muon), Phys. Lett. **B130**, 118 (1983).
[10] M. Arneodo *et al.* (European Muon), Z. Phys. **C34**, 277 (1987).
[11] M. R. Adams *et al.* (E665), Phys. Rev. **D48**, 5057 (1993).
[12] J. Breitweg *et al.* (ZEUS), Phys. Lett. **B481**, 199 (2000), `arXiv:hep-ex/0003017` .
[13] A. Airapetian *et al.* (HERMES Collaboration), Phys.Rev. **D87**, 012010 (2013), `arXiv:1204.4161[hep-ex]` .
[14] C. Adolph *et al.* (COMPASS), Nucl. Phys. **B886**, 1046 (2014), `arXiv:1401.6284[hep-ex]` .
[15] M. Boglione, S. Melis, and A. Prokudin, Phys.Rev. **D84**, 034033 (2011), `arXiv:1106.6177[hep-ph]` .
[16] B. Mecking *et al.* (CLAS Collaboration), Nucl. Instrum. Meth. **A503**, 513 (2003).
[17] H. Avakian *et al.* (CLAS Collaboration), Phys. Rev. Lett. **105**, 262002 (2010), `arXiv:hep-ex/1003.4549[hep-ex]` .
[18] A. Signori, A. Bacchetta, M. Radici, and G. Schnell, JHEP **1311**, 194 (2013), `arXiv:1309.3507[hep-ph]` .
[19] I. Akushevich, N. Shumeiko, and A. Soroko, Eur. Phys. J. **C10**, 681 (1999), `arXiv:hep-ph/9903325` .
[20] I. Akushevich, A. Ilyichev, and M. Osipenko, Phys.Lett. **B672**, 35 (2009), `arXiv:0711.4789[hep-ph]` .
[21] N. Harrison, H. Avakian, and K. Joo, *Proceedings, 24th International Workshop on Deep-Inelastic Scattering and Related Subjects (DIS 2016): Hamburg, Germany, April 11-15, 2016*, PoS **DIS2016**, 215 (2016).
[22] M. Osipenko *et al.* (CLAS), Phys. Rev. **D80**, 032004 (2009), `arXiv:hep-ex/0809.1153[hep-ex]` .
[23] M. Anselmino *et al.*, Phys. Rev. **D71**, 074006 (2005), `arXiv:hep-ph/0501196` .
[24] Y. Prok *et al.* (CLAS), Phys. Rev. **C90**, 025212 (2014), `arXiv:1404.6231[nucl-ex]` .
[25] C. Bourrely and J. Soffer, Nucl. Phys. **A941**, 307 (2015), `arXiv:1502.02517[hep-ph]` .
[26] M. Anselmino, V. Barone, and A. Kotzinian, Phys. Lett. **B706**, 46 (2011), `arXiv:1109.1132[hep-ph]` .
[27] M. Anselmino, V. Barone, and A. Kotzinian, Phys. Lett. **B699**, 108 (2011), `arXiv:1102.4214[hep-ph]` .
[28] H. Avakian and S. Pisano, *Proceedings, 24th International Workshop on Deep-Inelastic Scattering and Related Subjects (DIS 2016): Hamburg, Germany, April 11-15, 2016*, PoS **DIS2016**, 214 (2016).
[29] T. Navasardyan *et al.*, Phys. Rev. Lett. **98**, 022001 (2007), `arXiv:hep-ph/0608214` .